HHS Public Access

Author manuscript

Transbound Emerg Dis. Author manuscript; available in PMC 2024 March 25.

Published in final edited form as:

Transbound Emerg Dis. 2022 September ; 69(5): e2563–e2577. doi:10.1111/tbed.14602.

Modelling the ecological niche of naturally occurring anthrax at global and circumpolar extents using an ensemble modelling framework

Mark A. Deka,

Antonio R. Vieira,

William A. Bower

Centers for Disease Control and Prevention, Atlanta, Georgia, USA

Abstract

Bacillus anthracis, the causative agent of anthrax, is a spore-forming bacterium that primarily affects herbivorous livestock, wildlife and humans exposed to direct contact with infected animal carcasses or products. To date, there are a limited number of studies that have delineated the potential global distribution of anthrax, despite the importance of the disease from both an economic and public health standpoint. This study compiled occurrence data (n = 874) of confirmed human and animal cases from 1954 to 2021 in 94 countries. Using an ensemble ecological niche model framework, we developed updated maps of the global predicted ecological suitability of anthrax to measure relative risk at multiple scales of analysis, including a model for circumpolar regions. Additionally, we produced maps quantifying the disease transmission risk associated with anthrax to cattle, sheep and goat populations. Environmental suitability for *B. anthracis* globally is concentred throughout Eurasia, sub-Saharan Africa, the Americas, Southeast Asia, Australia and Oceania. Suitable environments for *B. anthracis* at the circumpolar scale extend above the Arctic Circle into portions of Russia, Canada, Alaska and northern Scandinavia. Environmental factors driving *B. anthracis* suitability globally include vegetation, land surface temperature, soil characteristics, primary climate conditions and topography. At the circumpolar scale, suitability is influenced by soil factors, topography and the derived climate characteristics. The greatest risk to livestock is concentrated within the Indian subcontinent, Australia, Anatolia, the Caucasus region, Central Asia, the European Union, Argentina, Uruguay, China, the United States, Canada and East Africa. This study expands on previous work by providing enhanced knowledge of the potential spatial distribution of anthrax in the Southern Hemisphere, sub-Saharan Africa, Asia and circumpolar regions of the Northern Hemisphere. We conclude that these updated

Correspondence: Mark A. Deka, Centers for Disease Control and Prevention, 1600 Clifton Rd, Atlanta, GA 30333, USA. pmu5@cdc.gov.

CONFLICT OF INTEREST

The authors declare that the research was conducted in the absence of any commercial or financial relationships that could be construed as a potential conflict of interest. The findings and conclusions in this document are those of the authors and do not necessarily represent the views of the Centers for Disease Control and Prevention.

ETHICS STATEMENT

The authors confirm that the ethical policies of the journal, as noted on the journal's author guidelines page, have been adhered to.

SUPPORTING INFORMATION

Additional supporting information can be found online in the Supporting Information section at the end of this article.

maps will provide pertinent information to guide disease control programs, inform policymakers and raise awareness at the global level to lessen morbidity and mortality among animals and humans located in environmentally suitable areas.

Keywords

anthrax; ensemble ecological niche modelling; epidemiology; precision mapping

1 | INTRODUCTION

Bacillus anthracis, the causative agent of anthrax, is a gram-positive, rod-shaped and spore-forming bacterium that primarily affects herbivorous livestock and wildlife and is usually fatal among these animals (Fasanella et al., 2010; Shadomy & Smith, 2008; WHO, 2008). Humans can acquire anthrax via cutaneous, ingestion, inhalation or injection routes. Most human cases are associated with direct contact with infected carcasses or contaminated animal products and can result in significant public health impacts if not correctly diagnosed and treated. In addition, *B. anthracis* spores can survive in the environment for long periods, resulting in recurrent contamination of livestock and the existence of high-risk areas for anthrax outbreaks (Hugh-Jones & Blackburn, 2009; Romero-Alvarez et al., 2020; Schmid & Kaufmann, 2002). Although the disease is distributed worldwide, it is endemic to Africa, the Middle East, South America and Central Asia, where outbreaks cause substantial public health and economic burdens (Hugh-Jones & Blackburn, 2009; Shadomy et al., 2016; Sushma et al., 2021). Furthermore, in endemic, low-resource areas, anthrax outbreaks in livestock often lead to secondary human infections through the practice of slaughtering sick animals to recoup income or food from lost animals (Bengis & Frean, 2014; Misgie et al., 2015).

Spatial modelling of disease distribution can help identify and predict high-risk areas for infectious diseases (Gangnon & Clayton, 2000; Peterson, 2006). Several approaches have been used to explore and predict the geographic distribution of suitable environments under which potential spore survival and possible anthrax transmission may occur (Kracalik et al., 2012; Otieno et al., 2021). Anthrax risk maps created by ecological niche modelling (ENM) are critical tools for understanding the epizootiology of the disease and prioritising areas for interventions. ENM is a quantitative technique that links occurrence data with remotely sensed environmental coverages, allowing for developing a correlative model of relative suitability for a pathogen. This approach has been previously used to estimate the spatial distributions of multiple pathogens at global and regional scales. For example, previous anthrax ENMs have estimated the distribution of *B. anthracis* in places like the United States, Australia, Central Africa and globally (Barro et al., 2016; Blackburn et al., 2007; Carlson et al., 2019; Chikerema et al., 2013; Mullins et al., 2013). These studies have regularly shown associations between *B. anthracis* spore survival and environmental factors such as soil organic matter concentration, soil pH, calcium concentrations and climatic conditions.

Ensemble ENM combines information from multiple individual models to predict an outcome. Ensemble forecasting enables a more robust model that can overcome the inherent uncertainties derived from each model by including multiple modelling algorithms (Sharma et al., 2021). This approach has been used in health research for the burden of disease estimates and, more recently, to predict disease spatial and temporal distribution (Bannick et al., 2020; Ray & Reich, 2018). In this study, we expand on previous work performed to predict the potential global ecological niche of anthrax by exploring the relationship between occurrence locations and environmental factors via an ensemble ENM framework. In addition, due to the emergence of anthrax in the Arctic region associated with climate change and melting permafrost (Stella et al., 2020), this study also provided an update to the potential ecological niche of anthrax in circumpolar areas. Furthermore, we quantified the disease transmission risk to cattle, goat and sheep populations globally by combining our niche modelling methodology with livestock density data. Previous studies have applied this risk mapping procedure to estimate exposure risk to infectious diseases (Alaniz et al., 2017, 2020; Carvajal et al., 2020). This information is critical to identifying areas for building veterinary and public health capacity to adequately prevent and respond to anthrax outbreaks in livestock, wildlife and humans.

2 | DATA AND METHODS

2.1 | Occurrence data

We assembled an occurrence dataset from a combination of human and animal cases and anthrax animal burial sites reported by ProMed Mail (https://promedmail.org/), laboratory-confirmed isolates of *B. anthracis*, published articles from Google Scholar (https://scholar.google.com/) and PubMed (https://pubmed.ncbi.nlm.nih.gov/) and geo-referenced data from digitized maps (please see Supporting Information Table S1). Search terms included, for example, ‘anthrax United States’, ‘anthrax Russia’, ‘anthrax Africa’, ‘anthrax animals’ and ‘anthrax human’. All types of studies were included. No time range or article type limits were applied. The compiled database totalled 874 records spanning 94 countries and a temporal range from 1954 to 2021. Before the modelling stage, we removed duplicate and spatially autocorrelated occurrence records by spatially filtering our dataset at a threshold of 50 km using the R programming language (Team R, 2013) package spThin (Aiello-Lammens et al., 2015). The final cleaned dataset contained 713 unique spatial locations. Spatial information for each site was manually georeferenced with Google Earth (https://earth.google.com/) and the OpenStreetMap Project (https://www.openstreetmap.org/#map=5/38.007/-95.844). Coordinates for these locations were standardized in a geographic coordinate system (WGS84) in ArcGIS Desktop 10.8.1. (ESRI. ArcGIS desktop: release 10.8.1. Environmental Systems Research Institute).

2.2 | Model calibration area (M)

The model calibration area or **M** region was delineated as point buffers of 250 km (Simoes et al., 2020). This step is an essential component of the general theory of niche modelling and corresponds to **M** in the biotic (B), abiotic (A), and movement (M) framework (Simoes et al., 2020; Soberón & Peterson, 2005). Previous work by Romero-Alvarez (2020) and colleagues implemented a similar calibration strategy in mapping the potential ecological

suitability of *B. anthracis* and *B. cereus biovar anthracis* in sub-Saharan Africa. The **M** region is the area within the broader background landscape that has 'likely' to have been tested by the species but is not completely occupied (Barve et al., 2011). Thus, the **M** region represents the hypothesized region in which a species can explore and colonize over time (Romero-Alvarez et al., 2020). ENMs can be susceptible to overinflation of evaluation metrics based on the choice of study area. For example, larger calibration areas tend to inflate evaluation metrics and bias conclusions (Barve et al., 2011; Simoes et al., 2020). The selection of **M** has a strong influence on model validation as demonstrated by Lobo et al. (2008). Lobo et al. (2008) highlight that during validation, areas outside of **M** will be predicted at lower suitability levels, and as a result, because of the inclusion of these areas, the model may display misleading evaluation statistics.

2.3 | Environmental predictors

Gridded environmental coverages represented climate and water balance data, soil characteristics, vegetation (EVI), land surface temperature (LST) and topographic features (Table 1). High-resolution climatological data were obtained from TerraClimate (1981—2010; http://www.climatologylab.org/terraclimate.html), a global repository of ecological and hydrological variables (Abatzoglou et al., 2018) at a 2.5 arc-min resolution. The TerraClimate dataset features monthly data for terrestrial surfaces and combines climatological normals from the WorldClim (Fick & Hijmans, 2017) dataset with time-varying data from CRU Ts4.0 and the Japanese 55-year Reanalysis (Abatzoglou et al., 2018). We chose not to incorporate the widely cited WorldClim database (Fick & Hijmans, 2017) in this study due to known spatial artefacts and uncertainties (Bobrowski et al., 2021; Escobar et al., 2014). The TerraClimate dataset is advantageous because of the inclusion of hydrological and surface hydrological process variables (Lemenkova, 2022).

These data were subsequently divided into their derived and primary characteristics for this analysis (http://www.climatologylab.org/terraclimate.html). The primary characteristics (Set 1) were the maximum (*t*max) and minimum temperature (*t*min), vapour pressure (*vap*), precipitation (*ppt*), downwards surface shortwave radiation (*srad*) and wind speed (*ws*). The derived variables (Set 2) include actual evapotranspiration (*aet*), potential evapotranspiration (*pet*), climate water deficit (*def*), soil moisture (*soil*), snow water equivalent (*swe*) and vapour pressure deficit (*vpd*). Gridded soil coverages were obtained from the Soil Grids (https://soilgrids.org/) database at a depth of 0–5 cm at a spatial resolution of 10 km (Set 3). These soil properties are identified as critical ecological predictors of *B. anthracis*, including soil pH (H_20 content), cation exchange capacity and organic carbon content (Carlson et al., 2019; Romero-Alvarez et al., 2020).

The Van Ness (1971) 'incubator area' hypothesis postulates that the ideal environment for spore germination exists under conditions of alkaline pH, soil moisture, the presence of organic matter and ambient air temperature above 15.5°C. Additionally, we included a moderate resolution imaging spectroradiometer (MODIS), enhanced vegetation index (EVI; ~1 km; mean monthly) and mean 8-day land surface temperature (LST) (~1 km) datasets (Set 4; Tomislav, 2018) from the WorldGrids archive (https://zenodo.org/record/1637816#.YmXwQOjMKUk). Vegetation biomass (EVI) and land surface temperature

(LST) are important variables when estimating the ecological niche of *B. anthracis* and various livestock-related diseases (Chikerema et al., 2013; Kracalik et al., 2013; Otieno et al., 2021; Suresh et al., 2022). We further considered topographic features: elevation and slope (Amatulli et al., 2018) (~10 km; Dragon & Rennie, 1995; Driciru et al., 2020; Van Ness, 1971; Set 5). Dragon and Rennie (1995) emphasize that the interaction between water, rainfall and topographic features can cause spore concentrations in low-lying areas. These would include bottomlands and the beds of creeks and rivers. We resampled all variables at a 10-km resolution to ensure a uniform cell size and processing extent using resampling and masking tools available in ArcGIS Desktop 10.8.1. (ESRI. ArcGIS desktop: release 10.8.1. Environmental Systems Research Institute; www.esri.com).

2.4 | Principal component analysis (PCA)

A PCA reduced multicollinearity and dimensionality between the environmental variables. The covariates were separated into five sets (Sets 1–5) to calculate the main principal components (PCs) using the cross-platform application Niche Analyst (Quio et al., 2016; http://nichea.sourceforge.net/). PCA is an orthogonal linear transformation that is used for both exploratory and predictive modelling (Joliffe, 2002). Here, a PCA was conducted for the environmental space defined by the **M** region and projected globally (Figure 1) and to circumpolar areas greater than 55° N latitude (Figure 2). Previous ENM studies have applied a similar two-step process for calibrating and projecting PCs to create new sets of orthogonal predictors (Alkishe & Peterson, 2021 ; Deka et al., 2022; Romero-Alvarez et al., 2020). For the TerraClimate dataset, the first four PCs were retained for the primary climate characteristics (98%), and the first five for the derived climate variables (97%). In addition, we retained three PCs for soil (100%) and two PCs for vegetation (EVI) and land surface temperature (LST) (100%), as well as elevation—slope (100%).

2.5 | Ecological niche modeling (ENM)

The ENMs presented in this study were created with the R programming language (Team R, 2013) package ‘biomod2’ (Thuiller et al., 2016). Biomod2 is an ensemble ENM platform that allows for the forecasting of species distributions with the application of multiple modelling techniques. This method reduces the predictive uncertainty that can occur due to intermodal variability by combining multiple models to determine dominant trends in the data (Elith & Graham, 2009). In total, eight algorithms were selected (8 × 10 replicates = 80 models): generalized boosted models (GBM;Elith et al., 2008), generalized additive models (GAM;Guisan et al., 2002), generalized linear models (GLM;Guisan et al., 2002), random forest (RF; Breiman, 2001), artificial neural networks (ANN; Lek & Guegan, 1999), classification tree analysis (CTA; Vayssieres et al., 2000), flexible discriminant analysis (FDA; Hastie, 1994) and multiple adaptive regression splines (MARS; Friedman, 1991).

Pseudoabsence (PA) data within the **M** region were generated with the ‘surface range envelope’ model, which selected random points outside of the suitable area estimated by a rectilinear surface envelope from the model presence sample (quantile = 0.025 – 95% confidence interval; Thuiller et al., 2016). Within **M**, because we are constraining our calibration region, we specified for the global ensemble a 1:1 ratio (713:713; presence/pseudoabsence) and a 2:1 ratio (presence/pseudoabsence; 75:150) for the circumpolar model

to account for the smaller dataset. Common mistakes associated with PA generation for ENM are often the choice of using an excessive number of PAs, compared to occurrences (Sillero & Barbosa, 2021). We chose to equally weight our presence and PA data for each model (i.e., the weighted sum of presence equals the weighted sum of absences) as recommended by Barbet-Massin et al. (2012). The application of pseudoabsences in ENM is well established in quantitative disease ecology (Bhatt et al., 2013; Carlson et al., 2019; Hassan et al., 2021; Pigott et al., 2014). Next, we specified that 80% of the data within the **M** region be assigned as a random sample, with the remaining 20% used for verifying the model using the area under the curve (AUC) of the receiver operating characteristic (ROC; Elith et al., 2011).

An ensemble evaluation metric threshold specified that only ROC values greater than 0.80 were to be included to construct the final ensembles. The ROC (AUC) ranges from 0 to 1 and is determined by a comparison of the null model with the randomly predicted AUC value equal to 0.50. Values greater than 0.75 are regarded as being sufficiently discriminatory and useful (Elith et al., 2011). Variable importance of the PC sets (Sets 1–5) was calculated through a shuffling process of a single variable within the dataset and the correlation of the model predictions with the initial (i) and shuffled data (ii). Values closer to 0 assume that the variable has no influence on the model (Dutra Silva et al., 2019). Thus, we ranked variables of greatest contribution to both the global and circumpolar ensembles based on their high to low scores (mean over 80 replicates). The global and circumpolar ensembles (median) were classified into four suitability classes: (1) very high, (2) high, (3) medium and (4) low risk (natural breaks - Jenks). We computed the coefficient of variation (CV; sd/median) from the ENM projections to account for uncertainty in our models. Higher CV values represent greater model uncertainty, while the lower the CV values, the less uncertainty is present. We further divided these values into four classifications: (1) low, (2) moderate, (3) high and (4) very high uncertainty (natural breaks - Jenks).

2.6 | Model evaluation

The partial ROC (pROC) (Peterson et al., 2008) metric (5% training omission error rate; E = 0.05, i.e., sensitivity > 0.95) was applied to evaluate model performance and prediction. Unlike the traditional ROC metric (Elith et al., 2011), the pROC accesses omission error for independent points and the predicted area suitable for the species. Partial AUC values are derived from the ratio between the AUC and the null expectations of the AUC. The corresponding pROC ratios thus range from 0–2 (values of 1 = random performance; Peterson, 2012; Peterson et al., 2008). Partial AUC ratios greater than 1 and closer to 2 indicate better model predictive performance. Bootstrapping was applied to test for statistical significance of the AUCs (compared to the null expectations) by resampling 50% of the available data with 1000 iterations. The pROC tests were conducted with the R programming language (Team R, 2013) package ENMGadgets (Barve & Barve, 2013).

2.7 | Quantifying zones of exposure risk for livestock

The disease transmission risk of *B. anthracis* was mapped by linking the ecological niche of the bacterium with the potentially exposed livestock population. These zones of exposure risk were based on two primary factors: (i) the potential environmental suitability of

B. anthracis and (ii) the density of cattle, goats and sheep (Alaniz et al., 2017, 2020; Carvajal et al., 2020). This methodology falls into the realm of precision public health, which integrates geolocated health information and maps to identify regions of elevated disease risk with a high degree of spatial accuracy (Osgood-Zimmerman et al., 2018; Reich & Haran, 2018). Gridded livestock density data for cattle, goats and sheep were obtained from the Food and Agricultural Organisation (FAO) of the United Nations Map Catalog (https://data.apps.fao.org/map/catalog/srv/eng/catalog.search#/home; ~10 km). The combined livestock data were first reclassified into four categories: null (< 1 animal/km^2), low (> 1–10 animals/km^2), medium (> 11–100 animals/km^2) and high (> 101 animals/km^2). For each category, new values were assigned: null = 0, low = 1, medium = 2, high = 3. We then reclassified the global ensemble model into four categories: null (0), low (1), medium (2) and high (3) with an equal interval classification type. Both grids were multiplied together using the Raster Calculator tool in ArcGIS 10.8.1 (ESRI. ArcGIS desktop: release 10.8.1. Environmental Systems Research Institute; www.esri.com). The risk map legend symbolizes exposure zones as: very high, high, medium, low and very low.

3 | RESULTS

We compiled 874 occurrences of anthrax from 94 countries spanning the period from 1954 to 2021 (see Supporting Information, Appendix Figure 1). The majority of the occurrence data (75%) were collected from Russia (115), China (87), the United States (65), Australia (60), India (42), Kazakhstan (41), Turkey (35), Canada (28), Argentina (24), France (19), Iran (18), New Zealand (17), Zimbabwe (16), Italy (15), Bangladesh (15), Indonesia (14), Namibia (11), Kyrgyzstan (11), Kenya (10) and Chad (10). Model evaluation tests using the pROC approach determined that both ensembles yielded predictions above the null expectations. The global model had an average pROC ratio value of 1.57 (max: 1.73, min: 1.51), while the circumpolar model had an average pROC ratio score of 1.69 (max: 1.84, min: 1.46). The algorithm's predictive performance for the global ensemble was highest among the GBM, RF, GAM and FDA algorithms. Traditional ROC scores for GBM ranged from 0.859 to 0.796, RF: 0.849 to 0.797; GAM: 0.844 to 0.782 and FDA: 0.836 to 0.753. Additionally, MARS (0.834–0.764), ANN (0.831–0.762), GLM (0.826–0.753) and CTA (0.794–0.681) also displayed good overall predictive performance. Algorithm statistics for the circumpolar ensemble favored ANN (0.821–0.557), GBM (0.82–0.631), FDA (0.812–0.507), GLM (0.804–0.602) and RF (0.803–0.589). The algorithms with lower ROC scores were CTA (0.799–0.524), MARS (0.796–0.473) and GAM (0.729–0.554).

The global ensemble predicted well-established enzootic regions and those without reported human or animal cases (Figure 3). These areas occupy a broad geographic extent in the Northern and Southern Hemispheres. Hotspots in North America are prevalent throughout the Great Plains, Great Lakes region, central-southern California, Rocky Mountains, Pacific Northwest, Northwest Territories, Alberta and Saskatchewan. Suitability in Latin America is concentrated throughout Mexico, the Caribbean, northern Venezuela, Peru, Ecuador, Chile, Bolivia, Argentina, Uruguay and eastern Brazil. Our model predicted much of the known distribution of anthrax in Africa throughout the Sahel, South Sudan, Central African Republic, Cameroon, Nigeria, Ghana, Burkina Faso, Mali, the Ethiopian Highlands, Horn of Africa, African Great Lakes Region, Zambia, Zimbabwe, Namibia, South Africa and

Angola. Suitability throughout Eurasia is extensive within eastern and western Europe, the Anatolian Peninsula, Kazakhstan, eastern and western China, the Caucasus region, Iran and eastern Siberia. Moreover, the majority of the Indian Subcontinent (India, Pakistan, Bangladesh, Nepal) is predicted to be suitable for *B. anthracis* as was Southeast Asia (Thailand, Cambodia, Vietnam, Laos), Japan, the Philippines, Indonesia and the Korean Peninsula. Suitability in Australia is prevalent throughout the eastern and northern extents, as well as the south and southwest of the continent. The distribution of CV values corresponds with areas of predicted very high and high ecological suitability within North and South America, sub-Saharan Africa, Eurasia, Southeast Asia and Australia (see Supporting Information, Appendix Figure 2).

In contrast, the circumpolar model (Figure 4) highlighted suitability throughout Alaska, the Northwest Territories, Nunavut and the Great Slave and Great Bear Lake region, which had previously been known for anthrax epidemics among bison (Dragon & Rennie, 1995; Figure 4). Furthermore, the circumpolar model highlighted suitable environments within Norway, Finland, western–eastern Russia and the natural boundaries of the Lena River, Eastern Highlands, Kolyma Mountains and the Kamchatka Peninsula. The Ob River area and the Yamal Peninsula, the site of the 2016 anthrax outbreak, adjacent to the Gulf of Ob and the Kara Sea, were also deemed suitable for *B. anthracis*. The distribution of CV values corresponds with areas of ecological suitability (very high, high; see Supporting Information: Appendix Figure 3). Lower uncertainty values in the environment are distributed throughout northern Scandinavia, eastern–western Russia, northern and eastern Canada and Alaska.

Variable importance for the global ensemble was highest for vegetation (EVI) and land surface temperature (LST) (Set 4; PC1–22.693; PC2–16.584), soil characteristics (Set 3; soil pH, cation exchange capacity, organic carbon content; PC1–21.689; PC2–15.277), primary climate conditions (PC1–10.25; *t*max*, t*min*, vap, ppt, srad, ws*) and topography (elevation–slope; Set 5; PC1–5.19). The circumpolar model was most influenced by soil characteristics (Set 3; PC2–23.29; PC3–15.86; soil pH, cation exchange capacity, organic carbon content), topography (Set 5; PC1–14.107), derived climate (Set 2; *q, pet, aet, def, soil, swe, vpd;* PC2–13.43; PC1–11.98), vegetation (EVI) and land surface temperature (LST) (Set 4; PC1–12.087) as well as the primary climate characteristics (Set 1; Set 1; *t*max*, t*min*, vap, ppt, srad, ws*; PC2–10.334; PC1–10.03; Figure 5).

3.1 | *Bacillus anthracis* risk zones for livestock

The potential disease transmission risk to livestock (cattle, goats, sheep) globally is presented in Figure 6. Geographically, livestock is at risk throughout the Plains of Canada, the United States and much of Central America, stretching into Columbia, Venezuela, Peru and Ecuador. High-risk zones are pronounced in northern Argentina, northeastern Brazil and the Central Valley region in Chile. The risk to livestock on the African continent is extensive throughout the Sahel, the Horn of Africa, the African Great Lakes region, western Madagascar and Southern Africa, specifically Angola, South Africa, Botswana and Zimbabwe. Throughout Eurasia, disease transmission risk to livestock is widespread within the European Union, Anatolia, the Caucasus region, Southern Russia, northern

Mongolia, Kazakhstan, Uzbekistan, Tajikistan and Kyrgyzstan. In addition, similar to the global ensemble, much of the Indian subcontinent, including Bangladesh, northern Pakistan, and southern Nepal, has a medium to high-risk level for livestock populations. In East Asia, the risk to livestock is significant throughout western, northeastern, central and southeastern China, the Korea Peninsula, Japan, the Philippines, Vietnam, Cambodia, Thailand and Myanmar. Suitability within Indonesia is primarily confined to Java, Sumatra and Celebes. The threat to livestock in Australia is limited to New South Wales, Victoria, Queensland and Western Australia.

4 | DISCUSSION

Using an ensemble ENM framework, this research expanded our knowledge of the potential geographic range of *B. anthracis* at global and circumpolar extents. The results of this study indicate that the distribution of anthrax is tied to well-known regions with historical and contemporary human and animal cases throughout North, Central and South America, sub-Saharan Africa, eastern and northern China, Central Asia, eastern and western Europe, India, Australia and Southeast Asia. Global anthrax occurrence records were collected from 1954 to 2021 ($n = 874$) across 94 countries. This study provides an update to the global and circumpolar predicted suitability of anthrax as well as the estimated spatial risk to livestock populations. Our results suggest that globally, factors driving *B. anthracis* suitability include vegetation (EVI), land surface temperature (LST), soil characteristics (soil pH, cation exchange capacity and carbon content), primary climate conditions (*t*max*, t*min*, vap, ppt, srad, ws*) and topography (elevation and slope). However, at the circumpolar scale, suitability for *B. anthracis* is influenced to a greater degree by soil factors (soil pH, cation exchange capacity and carbon content), topography (elevation and slope) and the derived climate characteristics (*q, pet, aet, def, soil, swe, vpd*). Our results align with previous studies documenting the sensitivity of *B. anthracis* spores to environmental factors such as vegetation, soil pH, carbon content, geological features and temperature (Dragon & Rennie, 1995; Kracalik et al., 2017; Otieno et al., 2021; Walsh et al., 2018; WHO, 2008).

The risk of anthrax to livestock populations globally was (Figures 7–9) based on two primary factors: potential ecological suitability and livestock density (cattle, goats, sheep). This precision mapping framework has proven helpful in understanding the spatial risk factors associated with Zika virus and the pathogen *Cryptococcus* (Alaniz et al., 2017, 2020) at continental and global scales. Disease transmission risk for livestock is significant throughout the Great Plains of Canada and the United States, Central America, northeastern Brazil, the Pampas and Gran Chaco regions of Argentina and central Chile. The risk to livestock on the African continent is concentrated throughout the Sahel, the Horn of Africa, East Africa and Southern Africa; as well as the European Union, Anatolia, the Levant, Caucasus region, Mongolia and Central Asia. The risk to livestock is widespread throughout the Indian subcontinent, as well as East and Southeast Asia, Indonesia, the Philippines and western (Western Australia) and eastern Australia (Queensland, New South Wales, Victoria).

Previous literature linking anthrax outbreaks with ecological determinants is primarily regional and ranges from the contiguous United States, Central Asia, India, Australia, sub-Saharan Africa, China, Zimbabwe and Uganda (Barro et al., 2016; Blackburn et al.,

2007; Driciru et al., 2020; Joyner et al., 2010; Romero-Alvarez et al., 2020; Walsh et al., 2019). The ENM algorithms applied in these studies favoured the genetic algorithm of rule set prediction, Maxent and boosted regression trees (BRT) (Blackburn et al., 2015; Carlson et al., 2019; Chikerema et al., 2013). More recently, Assefa et al. mapped the environmental suitability of anthrax in Ethiopia with an ensemble ecological niche model (Assefa et al., 2020). To date, three articles have modelled the broad-scale distribution of anthrax globally and at higher northern latitudes (Carlson et al., 2019; Stella et al., 2021; Walsh et al., 2018).

Walsh and colleagues (2018) model highlighted potentially suitable environments for anthrax in circumpolar regions. This work used the Maxent algorithm (Phillips et al., 2006) and was particularly relevant considering the 2016 anthrax outbreak in the Yamal Peninsula, Russia, an outbreak affecting humans and wildlife, leading to the culling of thousands of reindeer (*Rangifer tarandus*) and significant economic loss to the local population (Hueffer et al., 2020). Walsh (2018) and colleagues concluded that warming temperatures, cattle density and wild ungulate species richness influenced the potential distribution at higher latitudes. Similar to Walsh (2018), Stella et al. (2021) applied Maxent (Phillips et al., 2006) in high-latitude regions of the Northern Hemisphere. They found that anthrax's potential diffusion and emergence were related to environmental factors such as the soil-temperature anomaly (T) and active layer permafrost thickness.

Carlson et al. (2019), employing BRT, produced the sole global distribution model of anthrax and found that soil characteristics such as soil pH and vegetation were responsible for driving suitability patterns. Although all three models offer a significant contribution to the literature on the disease ecology of anthrax, there is an ever-increasing demand to refine the known distribution of the disease. Thus, expanding on the previous work of Carlson et al. (2019), Walsh et al. (2018) and Stella et al. (2021), this study redefined anthrax's potential global and circumpolar distribution by exploring the relationship between occurrence locations and environmental factors via an ensemble ENM approach. Our models predicted an increase in suitable environments in South America, sub-Saharan Africa, East Africa, Pakistan, Australia, India, East Asia, Southeast Asia and western Siberia. In addition to the work of Walsh (2018) and Stella (2021) and their current modelling scenario, our model predicted an increase in suitable environments in western Siberia, the Yamal Peninsula, Canada, Alaska, eastern Russia and northern Scandinavia.

Underlying the risk of re-emergence of anthrax in the Arctic is the increase in global temperatures and the thawing of active layers of permafrost (Stella et al., 2020). Anthropogenic-driven climate change in temperate and high latitude regions of North America and the Arctic is hypothesized to be the catalyst for warmer temperatures, more rainfall, droughts and extreme weather events (Kangbai & Momoh, 2017). These climate-related events play a central role in the incidence and distribution of emerging infectious diseases (Flahault et al., 2016). Regarding anthrax, because of its global distribution, it has been reported that climate change might promote a northern expansion of the disease. Thus, anthrax has been listed as a 'climate sensitive' disease (Parkinson et al., 2014; Stella et al., 2021; Walsh, de Smalen & Mor, 2018). Recent studies have brought to attention the risks associated with climate change in the Arctic and the potential reemergence of bacteria and viruses in not only permafrost but also deep layers of sea ice (Bradley et al., 2005; Hedlund

et al., 2014; Stella et al., 2021; Waits et al., 2018). With the emergence of anthrax in Yamal, Russia in 2016 (Hueffer et al., 2020) and Sweden (Agren et al., 2014), it is believed that thawing permafrost and the movement of spores through sediments and soil because of freeze–thaw cycles were the catalysts for spillovers in these events (Revich & Pobolnaya, 2011).

When comparing predicted high-risk anthrax areas estimated by this model versus estimates from other models, we observed a certain level of underprediction or lower capacity to detect risk areas by other models not using ensemble modelling. Overall, our global model suggests that anthrax spores could survive in much of the world and detected potentially endemic areas that had previously been under-predicted. Areas such as Northeast Brazil and parts of Southeast Asia, where no or few anthrax outbreaks have been reported. We hypothesize that the lack of disease surveillance and reporting could be responsible for the lack of data on anthrax occurrence in these areas. In regions where anthrax is not endemic, the disease is rarely recognized by human and animal health workers, where animal die-offs and human cases could easily be overlooked or misdiagnosed (WHO, 2008).

Ensemble ecological niche models are powerful tools that can be used to generate the most accurate predictions from incomplete and imperfect data. The flexibility of the ensemble modelling technique makes it a valuable tool for epidemiological questions, including disease mapping and niche modelling. Ensemble models use a range of components and perform better than single models alone (Bannick et al., 2020). Among the limitations of this study, it is essential to remember that ENM does not predict anthrax causation and is simply a correlative model, meaning that the spores may not be found in suitable areas. Also, ensemble models are more complex, and their interpretation is less direct than those provided by other modelling approaches. One risk of complex ensemble approaches is that they may overfit the data, resulting in models that place too much emphasis on one approach in a particular scenario or setting. Ray and Reich (2018) proposed using regularization or penalization to reduce the number of effective parameters estimated by a particular model as a helpful tool for ensemble infectious disease forecasting. However, due to the amount of data available and the ability to compare to previous models assessing the global distribution of anthrax, the risk of overfitting is decreased. Future work could explore the impact of weighting when ensembling.

Additionally, when utilizing ENMs, the risk of over -or underprediction needs to be acknowledged in the context of this study. For example, what was apparent in the global model was that some over-prediction was evident in much of Northern Australia, a region of the country without prior anthrax cases. In addition, overpredictions are also visible in the Great Lakes region of the United States and Canada. To account for this clear bias in the ecological suitability model, we deemed it necessary also to map the risk to livestock, which has a significantly higher risk of exposure to *B. anthracis* when compared to humans. Similarly, some limitations to the livestock risk model need to be stated. The model does not account for different types of animal management, including vaccination rates, livestock biosecurity and herd management. Areas determined as high risk for livestock do not necessarily reflect areas with a high burden of the disease. Perhaps in Western Europe and the United States, where more advanced and modern techniques for agriculture and animal

production and disease prevention are likely responsible for the low disease incidence, even in an area deemed as constituting a high degree of disease transmission risk.

5 | CONCLUSION

In summary, this study provides an update to the predicted ecological suitability of anthrax at global and circumpolar extents and delineates areas of elevated disease transmission risk to livestock populations. These maps can be used to enhance our understanding of the eco-epidemiology of *B. anthracis* and inform public and national health authorities on areas for potential anthrax occurrence, allowing for prioritization of interventions and preventive measures. Future work would benefit from continued transdisciplinary collaborations to improve these maps and those developed at finer geographic scales. It is hoped that the results of this study will enhance geographically targeted activities in environmentally suitable areas, which are critical in the management of anthrax, and provide the prerequisite for baseline assessments for data-driven control programs in endemic regions.

Supplementary Material

Refer to Web version on PubMed Central for supplementary material.

ACKNOWLEDGEMENTS

This project was supported in part by an appointment to the Research Participation Program at the Centers for Disease Control and Prevention administered by the Oak Ridge Institute for Science and Education through an interagency agreement between the US Department of Energy and the Centers for Disease Control and Prevention.

DATA AVAILABILITY STATEMENT

The data that support the findings of this study are available in the supplementary material of this article.

REFERENCES

Abatzoglou JT, Dobrowski SZ, Parks SA, & Hegewisch KC (2018). TerraClimate, a high-resolution global dataset of monthly climate and climatic water balance from 1958–2015. Scientific Data, 5(1), 1–12. [PubMed: 30482902]

Ågren J, Finn M, Bengtsson B, & Segerman B (2014). Microevolution during an anthrax outbreak leading to clonal heterogeneity and penicillin resistance. PLoS One, 9(2), e89112. [PubMed: 24551231]

Aiello-Lammens ME, Boria RA, Radosavljevic A, Vilela B, & Anderson RP (2015). spThin: An R package for spatial thinning of species occurrence records for use in ecological niche models. Ecography, 38(5), 541–545.

Alaniz AJ, Bacigalupo A, & Cattan PE (2017). Spatial quantification of the world population potentially exposed to Zika virus. International Journal of Epidemiology, 46(3), 966–975. [PubMed: 28338754]

Alaniz AJ, Carvajal JG, Carvajal MA, Cogliati M, & Vergara PM (2020). Spatial quantification of the population exposed to Cryptococcus neoformans and Cryptococcus gattii species complexes in Europe: Estimating the immunocompetent and HIV/AIDS patients under risk. Risk Analysis, 40(3), 524–533. [PubMed: 31578757]

Alkishe A, & Peterson AT (2021). Potential geographic distribution of Ixodes cookei, the vector of Powassan virus. Journal of Vector Ecology, 46(2), 155–162. [PubMed: 35230020]

Amatulli G, Domisch S, Tuanmu M-N, Parmentier B, Ranipeta A, Malczyk J, & Jetz W (2018). A suite of global, cross-scale topographic variables for environmental and biodiversity modeling. Scientific Data, 5(1), 1–15. [PubMed: 30482902]

Assefa A, Bihon A, & Tibebu A (2020). Anthrax in the Amhara regional state of Ethiopia; spatiotemporal analysis and environmental suitability modeling with an ensemble approach. Preventive Veterinary Medicine, 184, 105155. [PubMed: 33002656]

Bannick MS, McGaughey M, & Flaxman AD (2020). Ensemble modelling in descriptive epidemiology: Burden of disease estimation. International Journal of Epidemiology, 49(6), 2065–2073.

Barbet-Massin M, Jiguet F, Albert CH, & Thuiller W (2012). Selecting pseudo-absences for species distribution models: How, where and how many? Methods in Ecology and Evolution, 3(2), 327–338.

Barro AS, Fegan M, Moloney B, Porter K, Muller J, Warner S, & Blackburn JK (2016). Redefining the Australian anthrax belt: Modeling the ecological niche and predicting the geographic distribution of Bacillus anthracis. PLoS Neglected Tropical Diseases, 10(6), e0004689. [PubMed: 27280981]

Barve N, & Barve V (2013). ENMGadgets: Tools for pre and post processing in ENM workflows https://Github.Com/Vijaybarve/ENMGadgets

Barve N, Barve V, Jiménez-Valverde A, Lira-Noriega A, Maher SP, Peterson AT, Soberón J, & Villalobos F (2011). The crucial role of the accessible area in ecological niche modeling and species distribution modeling. Ecological Modelling, 222(11), 1810–1819.

Bengis R, & Frean J (2014). Anthrax as an example of the One Health concept. Revue Scientifique et Technique (International Office of Epizootics), 33(2), 593–604. [PubMed: 25707186]

Bhatt S, Gething PW, Brady OJ, Messina JP, Farlow AW, Moyes CL, Drake JM, Brownstein JS, Hoen AG, & Sankoh O (2013). The global distribution and burden of dengue. Nature, 496(7446), 504–507. [PubMed: 23563266]

Blackburn JK, McNyset KM, Curtis A, & Hugh-Jones ME (2007). Modeling the geographic distribution of Bacillus anthracis, the causative agent of anthrax disease, for the contiguous United States using predictive ecologic niche modeling. American Journal of Tropical Medicine and Hygiene, 77(6), 1103–1110. [PubMed: 18165531]

Blackburn JK, Odugbo MO, Van Ert M, O'Shea B, Mullins J, Perrenten V, Maho A, Hugh-Jones M, & Hadfield T (2015). Bacillus anthracis diversity and geographic potential across Nigeria, Cameroon and Chad: Further support of a novel West African lineage. PLoS Neglected Tropical Diseases, 9(8), e0003931. [PubMed: 26291625]

Bobrowski M, Weidinger J, & Schickhoff U (2021). Is new always better? Frontiers in global climate datasets for modeling treeline species in the Himalayas. Atmosphere, 12(5), 543.

Bradley MJ, Kutz SJ, Jenkins E, & O'hara TM (2005). The potential impact of climate change on infectious diseases of Arctic fauna. International Journal of Circumpolar Health, 64(5), 468–477. [PubMed: 16440609]

Breiman L (2001). Random forests. Machine Learning, 45(1), 5–32.

Carlson CJ, Kracalik IT, Ross N, Alexander KA, Hugh-Jones ME, Fegan M, Elkin BT, Epp T, Shury TK, & Zhang W (2019). The global distribution of Bacillus anthracis and associated anthrax risk to humans, livestock and wildlife. Nature Microbiology, 4(8), 1337–1343.

Carvajal JG, Alaniz AJ, Carvajal MA, Acheson ES, Cruz R, Vergara PM, & Cogliati M (2020). Expansion of the emerging fungal pathogen Cryptococcus bacillisporus into America: Linking phylogenetic origin, geographical spread and population under exposure risk. Frontiers in Microbiology, 11, 2117. [PubMed: 32983073]

Chikerema S, Murwira A, Matope G, & Pfukenyi D (2013). Spatial modelling of Bacillus anthracis ecological niche in Zimbabwe. Preventive Veterinary Medicine, 111(1–2), 25–30. [PubMed: 23726015]

Deka MD, Marston CK, Garcia-Diaz J, Drumgoole R, & Traxler RM (2022). Ecological niche model of Bacillus cereus group isolates containing a homologue of the pXO1 anthrax toxin genes infecting metalworkers in the United States. Pathogens, 11(4), 1–12.

Dragon DC, & Rennie RP (1995). The ecology of anthrax spores: Tough but not invincible. The Canadian Veterinary Journal, 36(5), 295. [PubMed: 7773917]

Driciru M, Rwego IB, Ndimuligo SA, Travis DA, Mwakapeje ER, Craft M, Asiimwe B, Alvarez J, Ayebare S, & Pelican K (2020). Environmental determinants influencing anthrax distribution in Queen Elizabeth Protected Area, Western Uganda. Plos One, 15(8), e0237223. [PubMed: 32810178]

Dutra Silva L, Brito de Azevedo E, Vieira Reis F, Bento Elias R, & Silva L (2019). Limitations of species distribution models based on available climate change data: A case study in the Azorean forest. Forests, 10(7), 575.

Elith J, & Graham CH (2009). Do they? How do they? WHY do they differ? On finding reasons for differing performances of species distribution models. Ecography, 32(1), 66–77.

Elith J, Leathwick JR, & Hastie T (2008). A working guide to boosted regression trees. Journal of Animal Ecology, 77(4), 802–813. [PubMed: 18397250]

Elith J, Phillips SJ, Hastie T, Dudík M, Chee YE, & Yates CJ (2011). A statistical explanation of MaxEnt for ecologists. Diversity and Distributions, 17(1), 43–57.

Escobar LE, Lira-Noriega A, Medina-Vogel G, & Peterson AT (2014). Potential for spread of the white-nose fungus (Pseudogymnoascus destructans) in the Americas: Use of Maxent and NicheA to assure strict model transference. Geospatial Health, 9(1), 221–229. [PubMed: 25545939]

Fasanella A, Galante D, Garofolo G, & Jones MH (2010). Anthrax undervalued zoonosis. Veterinary Microbiology, 140(3–4), 318–331. [PubMed: 19747785]

Fick SE, & Hijmans RJ (2017). WorldClim 2: New 1-km spatial resolution climate surfaces for global land areas. International Journal of Climatology, 37(12), 4302–4315.

Flahault A, de Castaneda RR, & Bolon I (2016). Climate change and infectious diseases. Public Health Reviews, 37(1), 1–3. [PubMed: 29450043]

Friedman JH (1991). Multivariate adaptive regression splines. The Annals of Statistics, 19(1), 1–67.

Gangnon RE, & Clayton MK (2000). Bayesian detection and modeling of spatial disease clustering. Biometrics, 56(3), 922–935. [PubMed: 10985238]

Guisan A, Edwards TC Jr., & Hastie T (2002). Generalized linear and generalized additive models in studies of species distributions: Setting the scene. Ecological Modelling, 157(2–3), 89–100.

Hassan R, Simpson H, Cano J, Bakhiet S, Ganawa E, Argaw D, Newport MJ, Deribe K, & Fahal AH (2021). Modelling the spatial distribution of mycetoma in Sudan. Transactions of The Royal Society of Tropical Medicine and Hygiene, 115(10), 1144–1152. [PubMed: 34037803]

Hastie T, Tibshirani R, & Buja A (1994). Flexible discriminant analysis by optimal scoring. Journal of the American Statistical Association, 89(428), 1255–1270.

Hedlund C, Blomstedt Y, & Schumann B (2014). Association of climatic factors with infectious diseases in the Arctic and subarctic region–a systematic review. Global Health Action, 7(1), 24161. [PubMed: 24990685]

Hueffer K, Drown D, Romanovsky V, & Hennessy T (2020). Factors contributing to Anthrax outbreaks in the circumpolar north. EcoHealth, 17(1), 174–180. [PubMed: 32006181]

Hugh-Jones M, & Blackburn J (2009). The ecology of Bacillus anthracis. Molecular Aspects of Medicine, 30(6), 356–367. [PubMed: 19720074]

Jolliffe IT (2002). Principal component analysis for special types of data Springer.

Joyner TA, Lukhnova L, Pazilov Y, Temiralyeva G, Hugh-Jones ME, Aikimbayev A, & Blackburn JK (2010). Modeling the potential distribution of Bacillus anthracis under multiple climate change scenarios for Kazakhstan. PloS One, 5(3), e9596. [PubMed: 20231894]

Kangbai J, & Momoh E (2017). Anthropogenic climatic change risks a global anthrax outbreak: A short communication. Journal of Tropical Diseases, 5(244), 2.

Kracalik IT, Blackburn JK, Lukhnova L, Pazilov Y, Hugh-Jones ME, & Aikimbayev A (2012). Analysing the spatial patterns of livestock anthrax in Kazakhstan in relation to environmental factors: A comparison of local (Gi*) and morphology cluster statistics. Geospatial Health, 7(1), 111–126. [PubMed: 23242686]

Kracalik IT, Kenu E, Ayamdooh EN, Allegye-Cudjoe E, Polkuu PN, Frimpong JA, Nyarko KM, Bower WA, Traxler R, & Blackburn JK (2017). Modeling the environmental suitability of anthrax in Ghana and estimating populations at risk: Implications for vaccination and control. PLoS Neglected Tropical Diseases, 11(10), e0005885. [PubMed: 29028799]

Kracalik IT, Malania L, Tsertsvadze N, Manvelyan J, Bakanidze L, Imnadze P, Tsanava S, & Blackburn JK (2013). Evidence of local persistence of human anthrax in the country of Georgia associated with environmental and anthropogenic factors. PLoS Neglected Tropical Diseases, 7(9), e2388. [PubMed: 24040426]

Lek S, & Guégan J-F (1999). Artificial neural networks as a tool in ecological modelling, an introduction. Ecological Modelling, 120(2–3), 65–73.

Lemenkova P (2022). Data fusion strategy for mapping environment and climate variables of Brazil. Tecno-Lógica, 26(1), 15–34.

Lobo JM, Jiménez-Valverde A, & Real R (2008). AUC: a misleading measure of the performance of predictive distribution models. Global Ecology and Biogeography, 17(2), 145–151.

Misgie F, Atnaf A, & Surafel K (2015). A review on anthrax and its public health and economic importance. Academic Journal of Animal Diseases, 4(3), 196–204.

Mullins JC, Garofolo G, Van Ert M, Fasanella A, Lukhnova L, Hugh-Jones ME, & Blackburn JK (2013). Ecological niche modeling of Bacillus anthracis on three continents: Evidence for genetic-ecological divergence? PloS One, 8(8), e72451. [PubMed: 23977300]

Osgood-Zimmerman A, Millear AI, Stubbs RW, Shields C, Pickering BV, Earl L, Graetz N, Kinyoki DK, Ray SE, & Bhatt S (2018). Mapping child growth failure in Africa between 2000 and 2015. Nature, 555(7694), 41–47. [PubMed: 29493591]

Otieno FT, Gachohi J, Gikuma-Njuru P, Kariuki P, Oyas H, Canfield SA, Blackburn JK, Njenga MK, & Bett B (2021). Modeling the spatial distribution of anthrax in southern Kenya. PLoS Neglected Tropical Diseases, 15(3), e0009301. [PubMed: 33780459]

Parkinson AJ, Evengard B, Semenza JC, Ogden N, Børresen ML, Berner J, Brubaker M, Sjöstedt A, Evander M, & Hondula DM (2014). Climate change and infectious diseases in the Arctic: Establishment of a circumpolar working group. International Journal of Circumpolar Health, 73(1), 25163. [PubMed: 25317383]

Peterson AT (2006). Ecologic niche modeling and spatial patterns of disease transmission. Emerging Infectious Diseases, 12(12), 1822. [PubMed: 17326931]

Peterson AT (2012). Niche modeling: Model evaluation. Biodiversity Informatics, 8(1), 4300. 10.17161/bi.v8i1.4300

Peterson AT, Papeş M, & Soberón J (2008). Rethinking receiver operating characteristic analysis applications in ecological niche modeling. Ecological Modelling, 213(1), 63–72.

Phillips SJ, Anderson RP, & Schapire RE (2006). Maximum entropy modeling of species geographic distributions. Ecological Modelling, 190(3–4), 231–259.

Pigott DM, Golding N, Mylne A, Huang Z, Henry AJ, Weiss DJ, Brady OJ, Kraemer MU, Smith DL, & Moyes CL (2014). Mapping the zoonotic niche of Ebola virus disease in Africa. Elife, 3, e04395. [PubMed: 25201877]

Qiao H, Peterson AT, Campbell LP, Soberón J, Ji L, & Escobar LE (2016). NicheA: Creating virtual species and ecological niches in multivariate environmental scenarios. Ecography, 39(8), 805–813.

Ray EL, & Reich NG (2018). Prediction of infectious disease epidemics via weighted density ensembles. PLoS Computational Biology, 14(2), e1005910. [PubMed: 29462167]

Reich BJ, & Haran M (2018). Precision maps for public health. Nature, 555(7694), 32–33.

Revich BA, & Podolnaya MA (2011). Thawing of permafrost may disturb historic cattle burial grounds in East Siberia. Global Health Action, 4(1), 8482.

Romero-Alvarez D, Peterson AT, Salzer JS, Pittiglio C, Shadomy S, Traxler R, Vieira AR, Bower WA, Walke H, & Campbell LP (2020). Potential distributions of Bacillus anthracis and Bacillus cereus biovar anthracis causing anthrax in Africa. PLoS Neglected Tropical Diseases, 14(3), e0008131. [PubMed: 32150557]

Schmid G, & Kaufmann A (2002). Anthrax in Europe: Its epidemiology, clinical characteristics, and role in bioterrorism. Clinical Microbiology and Infection, 8(8), 479–488. [PubMed: 12197870]

Shadomy SV, & Smith TL (2008). Anthrax. Journal of the American Veterinary Medical Association, 233(1), 63–72. [PubMed: 18593313]

Shadomy S, Idrissi AE, Raizman E, Bruni M, Palamara E, Pittiglio C, & Lubroth J (2016). Anthrax outbreaks: A warning for improved prevention, control and heightened awareness. Rome (Italy), https://www.fao.org/3/i6124e/i6124e.pdf

Sharma N, Dev J, Mangla M, Wadhwa VM, Mohanty SN, & Kakkar D (2021). A heterogeneous ensemble forecasting model for disease prediction. New Generation Computing, 39(3–4), 701–715. [PubMed: 33424081]

Sillero N, & Barbosa AM (2021). Common mistakes in ecological niche models. International Journal of Geographical Information Science, 35(2), 213–226.

Simoes M, Romero-Alvarez D, Nuñez-Penichet C, Jiménez L, & Cobos ME (2020). General theory and good practices in ecological niche modeling: A basic guide. Biodiversity Informatics, 15(2), 67–68.

Soberón J, & Peterson AT (2005). Interpretation of models of fundamental ecological niches and species' distributional areas. Biodiversity Informatics, 2, 1–10.

Stella E, Mari L, Gabrieli J, Barbante C, & Bertuzzo E (2020). Permafrost dynamics and the risk of anthrax transmission: A modelling study. Scientific Reports, 10(1), 1–12. [PubMed: 31913322]

Stella E, Mari L, Gabrieli J, Barbante C, & Bertuzzo E (2021). Mapping environmental suitability for anthrax reemergence in the Arctic. Environmental Research Letters, 16(10), 105013.

Suresh K, Hemadri D, Patil S, Krishnamoorthy P, & Siju S (2022). Livestock disease forewarning monthly bulletin-March 2022. NADRES Bulletin, 10(1), 1–126.

Team RC (2013). R: A language and environment for statistical computing https://www.r-project.org/

Thuiller W, Georges D, Engler R, Breiner F, Georges MD, & Thuiller CW (2016). Package 'biomod2'. Species distribution modeling within an ensemble forecasting framework https://cran.r-project.org/web/packages/biomod2/biomod2.pdf

Tomislav H (2018). WorldGrids archived layers at 1 km to 20 km spatial resolution 10.5281/zenodo.1637816

Van Ness GB (1971). Ecology of Anthrax: Anthrax undergoes a propagation phase in soil before it infects livestock. Science, 172(3990), 1303–1307. [PubMed: 4996306]

Vayssières MP, Plant RE, & Allen-Diaz BH (2000). Classification trees: An alternative non-parametric approach for predicting species distributions. Journal of Vegetation Science, 11(5), 679–694.

Waits A, Emelyanova A, Oksanen A, Abass K, & Rautio A (2018). Human infectious diseases and the changing climate in the Arctic. Environment International, 121, 703–713. [PubMed: 30317100]

Walsh MG, de Smalen AW, & Mor SM (2018). Climatic influence on anthrax suitability in warming northern latitudes. Scientific Reports, 8(1), 1–9. [PubMed: 29311619]

Walsh MG, Mor SM, & Hossain S (2019). The elephant–livestock interface modulates anthrax suitability in India. Proceedings of the Royal Society B, 286(1898), 20190179. [PubMed: 30862290]

World Health Organization. (2008). International health regulations (2005) World Health Organization.

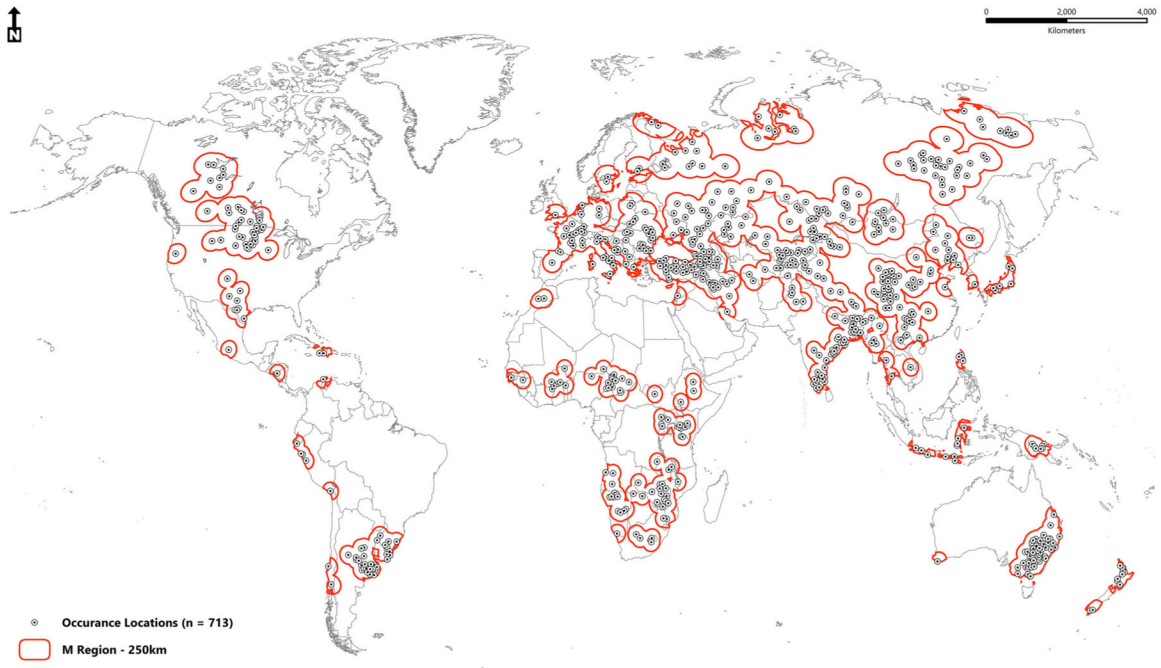

FIGURE 1.

Bacillus anthracis filtered (*n* = 713) occurrence records (white-black) buffered at 250 km (red) to define the model calibration (**M** region)

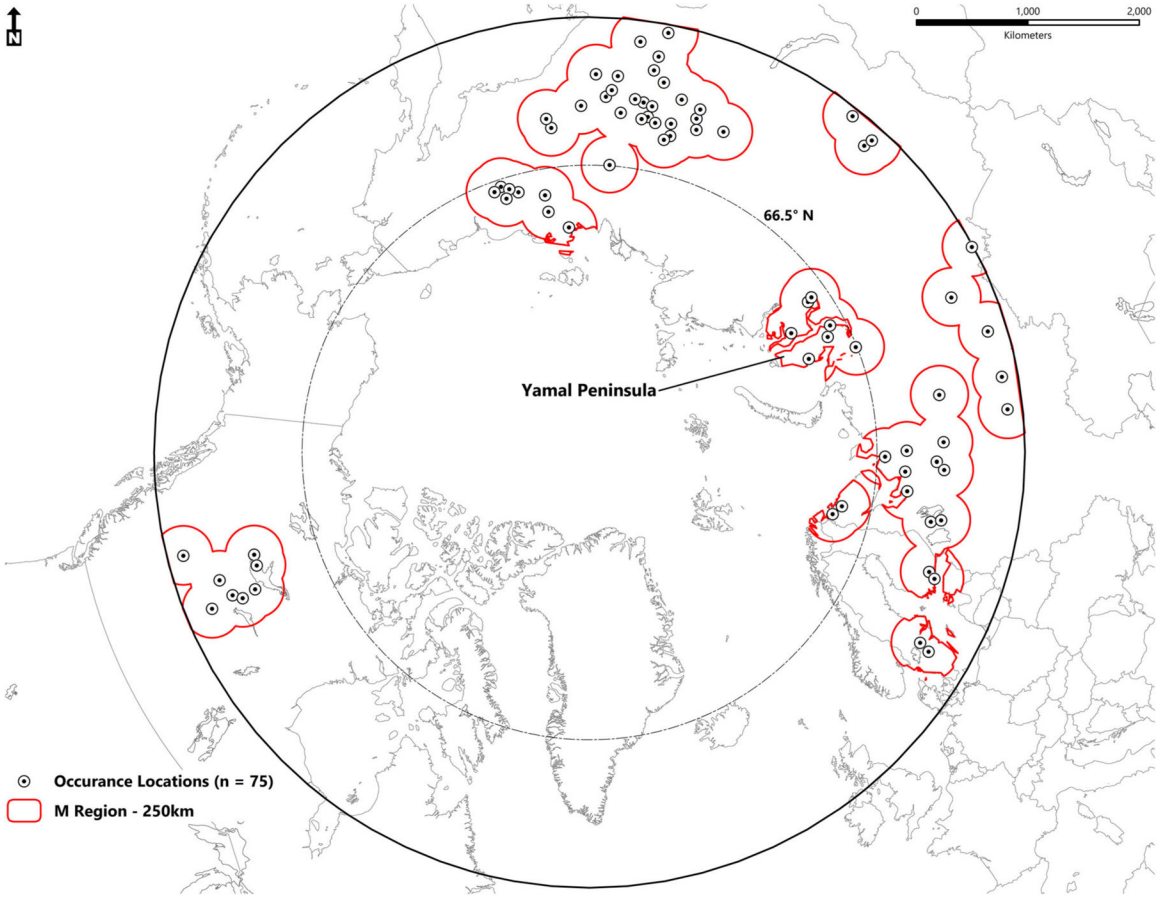

FIGURE 2.

Bacillus anthracis filtered (*n* = 75) occurrence records (white-black) buffered at 250 km (red) to define the model calibration (**M** region). The Yamal Peninsula (Russia), the site of the 2016 outbreak, is highlighted. The Arctic circle is represented at 66.5 N latitude

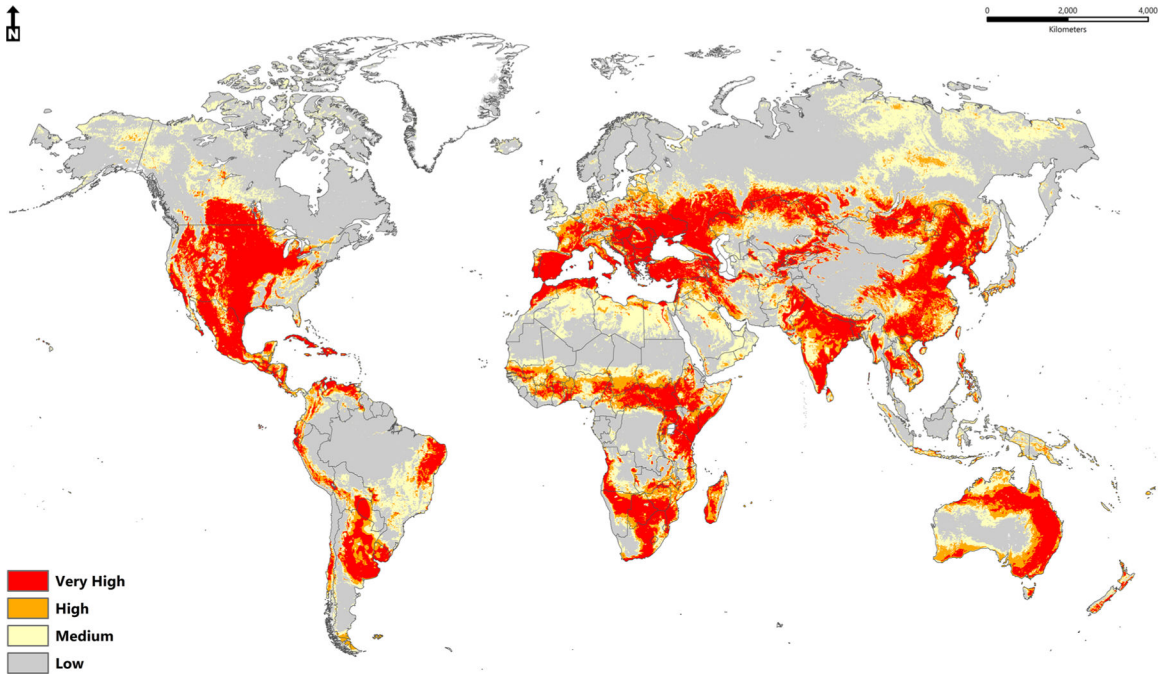

FIGURE 3.
Predicted global suitability of *B. anthracis* (median)

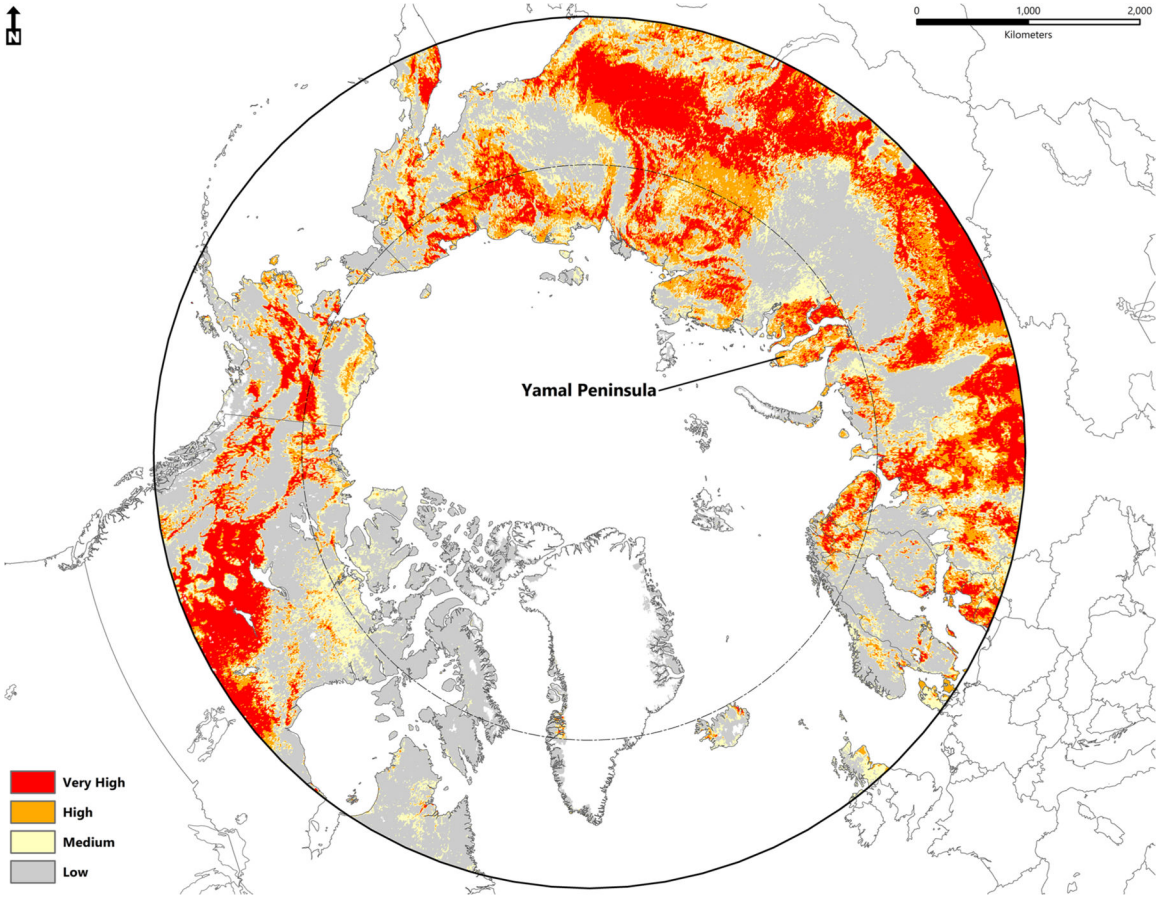

FIGURE 4.

Predicted circumpolar suitability of *B. anthracis*. Highlighted is the Yamal Peninsula (Russia), the site of the 2016 outbreak

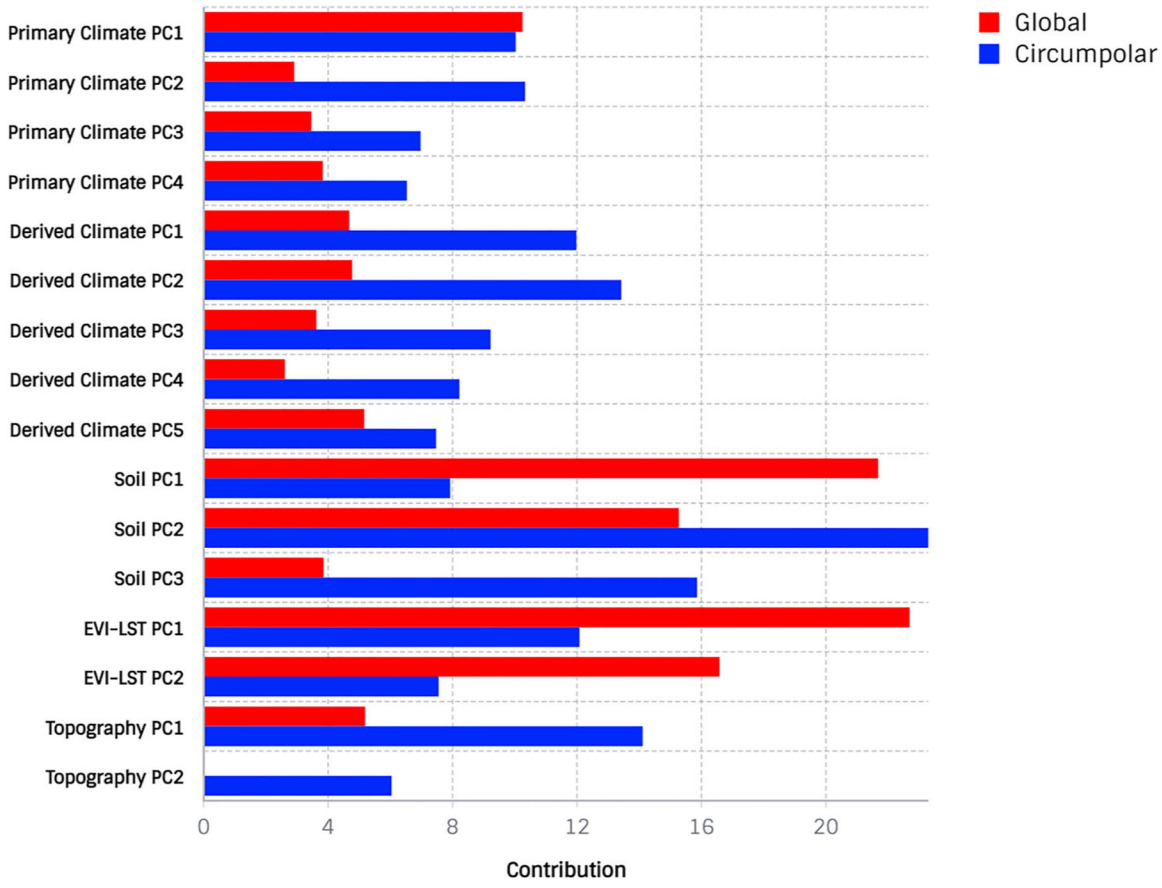

FIGURE 5.

Variable contribution for the principal component (PC) sets used for the global and circumpolar ensembles. Variables on the y-axis correspond to the PC sets

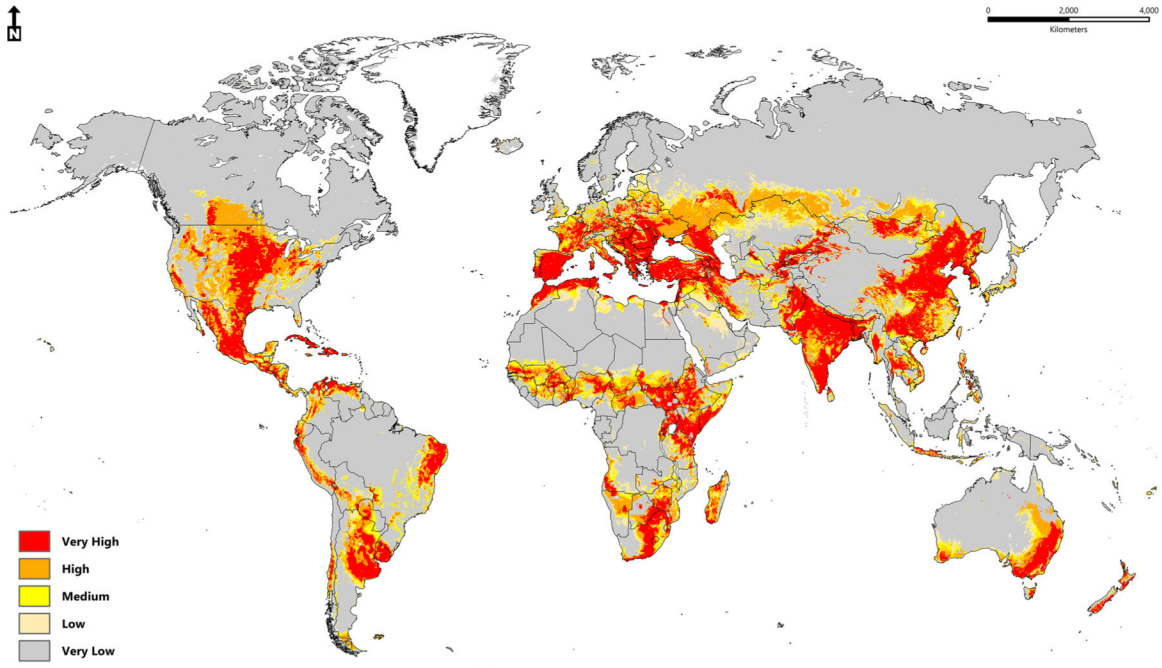

FIGURE 6.
Anthrax disease transmission risk globally (cattle, goats and sheep)

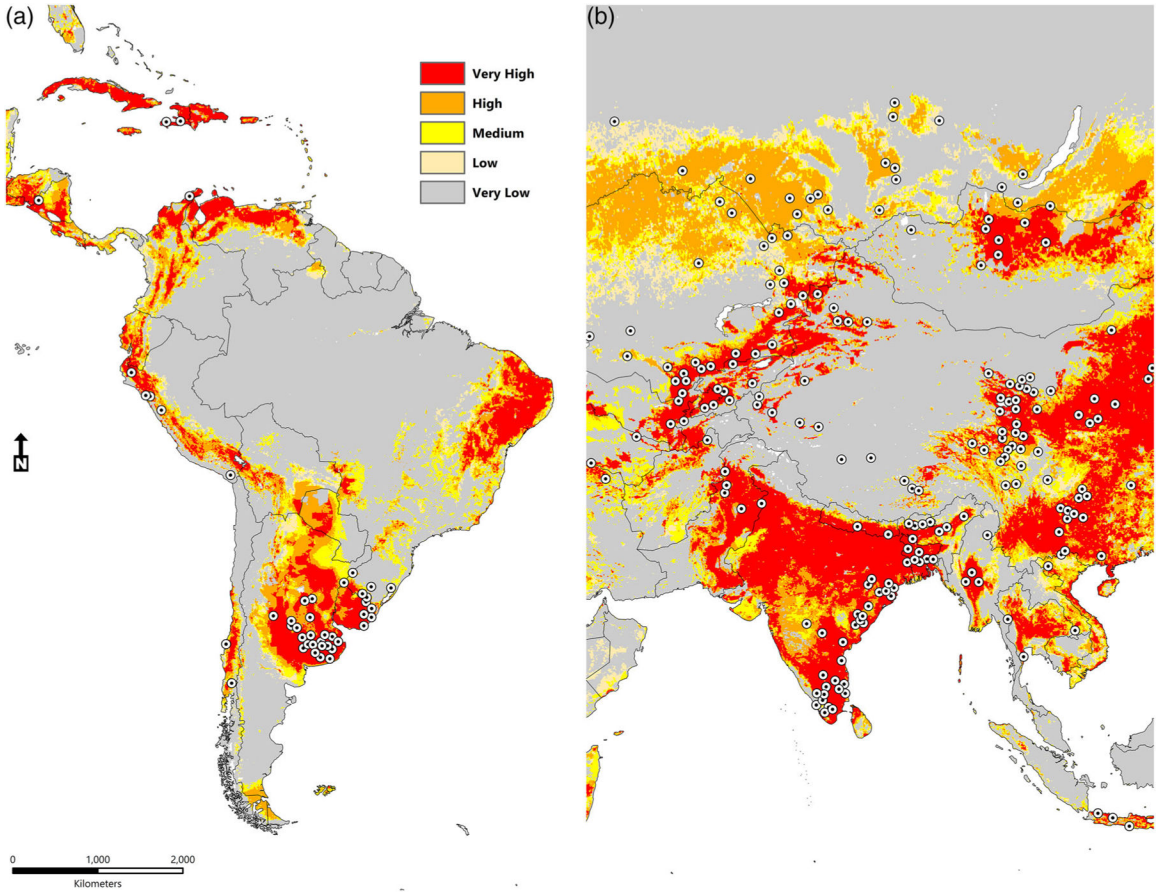

FIGURE 7.

Anthrax disease transmission risk (cattle, goats and sheep) in Latin America (a) and Central, South, Southeast and East Asia (b). White-black symbols represent anthrax occurrence records

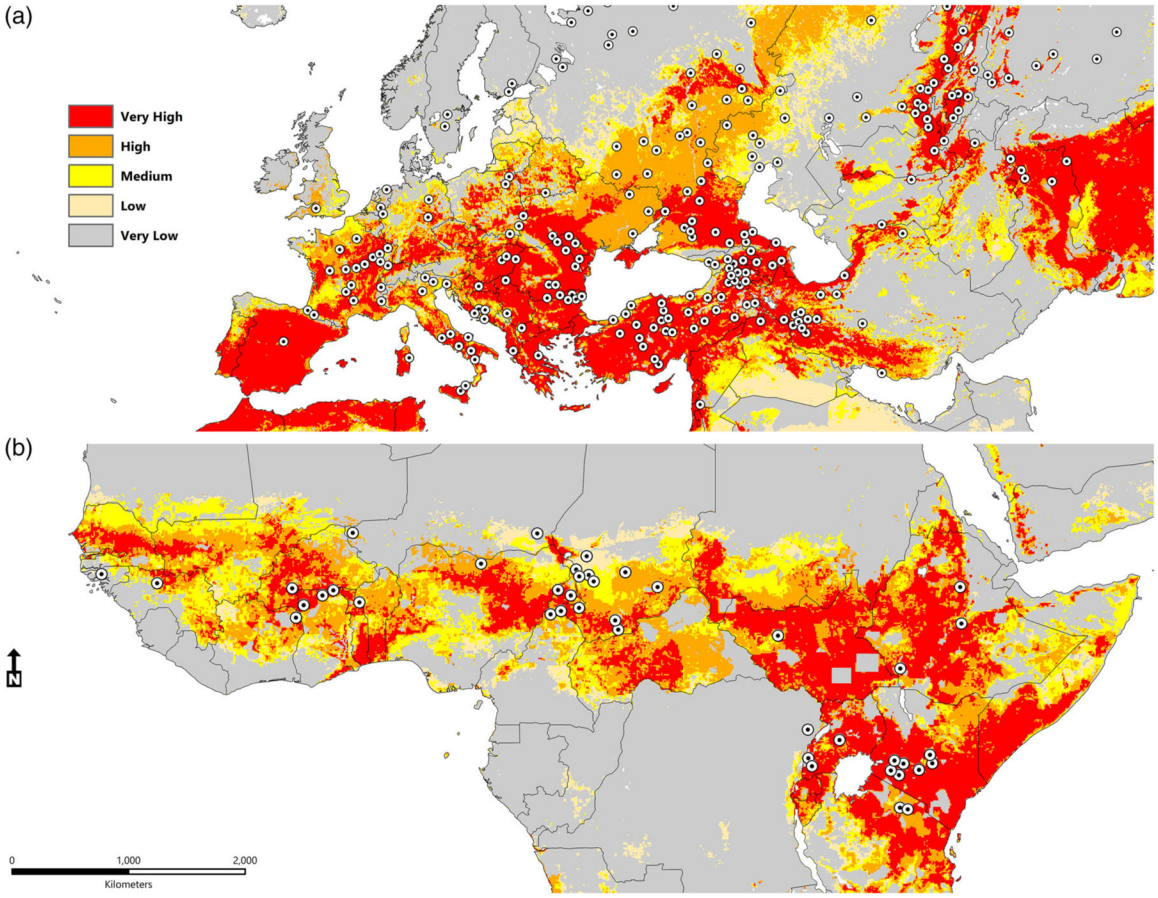

FIGURE 8.

Anthrax disease transmission risk (cattle, goats and sheep) in Eurasia (a) and sub-Saharan Africa (b). White-black symbols represent the anthrax outbreak occurrence records

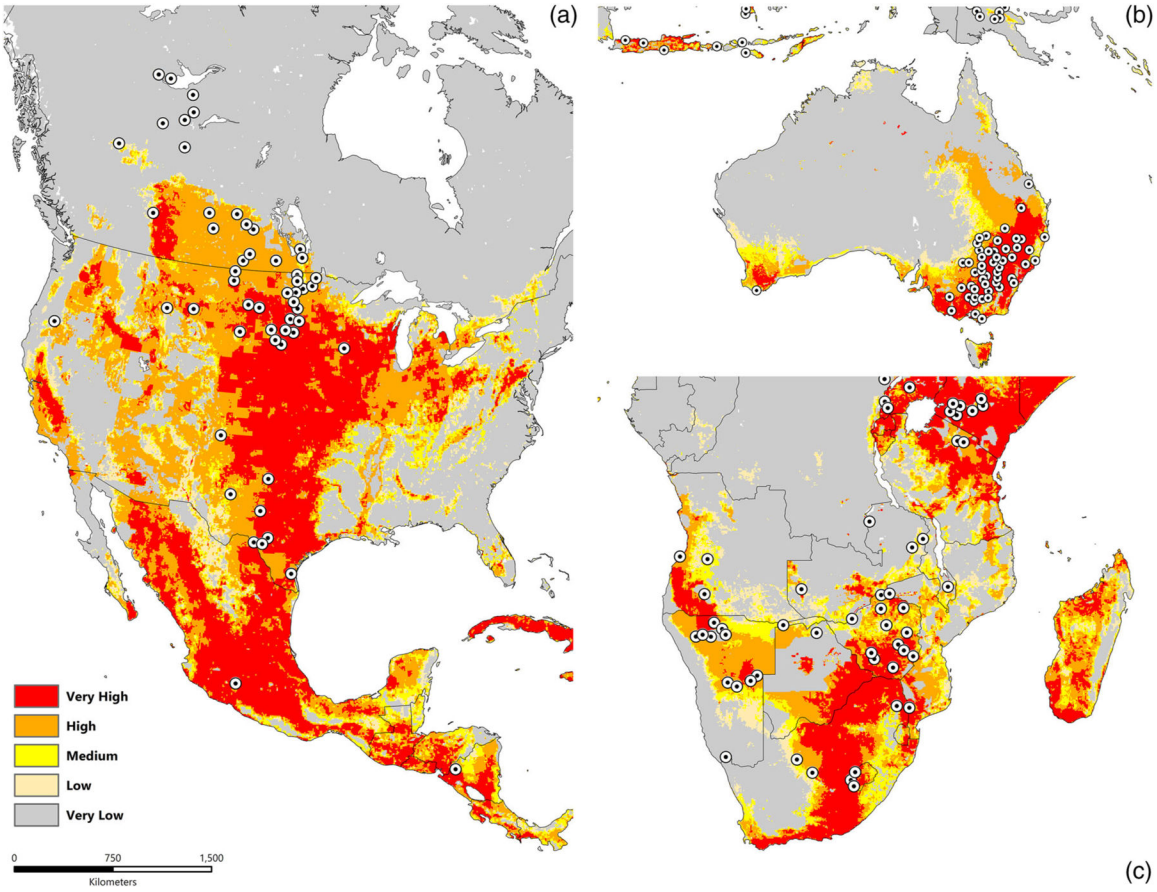

FIGURE 9.

Anthrax disease transmission risk (cattle, goats and sheep) in North and Central America (a), Australia (b) and Southern Africa (c). White-black symbols represent the anthrax outbreak occurrence records

TABLE 1

Environmental variables included in the ecological niche model at global and circumpolar extents

Primary climate variables (Set 1)	**Unit**	**Source**
*Maximum Temperature (*tmax)	°C	TerraClimate
*Minimum Temperature (*tmin)	°C	TerraClimate
Vapour Pressure (vap)	kPa	TerraClimate
Precipitation (ppt)	mm	TerraClimate
Downwards Surface Shortwave Radiation (srad)	w/m^2	TerraClimate
Wind Speed (ws; 1981–2010)	m/s	TerraClimate
Derived Climate Variables (Set 2)		
Runoff (q)	mm	TerraClimate
Potential Evapotranspiration (pet)		
Actual Evapotranspiration (aet)	mm	TerraClimate
Climate Water Deficit (def)	mm	TerraClimate
Soil Moisture (soil)	mm	TerraClimate
Snow Water Equivalent (swe)	mm	TerraClimate
Vapour Pressure Deficit (vpd)	kpa	TerraClimate
Soil Characteristics (Set 3)		
Soil pH (H_2O)	g/100 g	Soil Grids
Cation Exchange Capacity	g/100 g	Soil Grids
Organic Carbon	g/100 g	Soil grids
Vegetation and Surface Energy (Set 4)		
Enhanced Vegetation Index (EVI)	0–6.5	WorldGrids
Land Surface Temperature (LST)	°C	WorldGrids
Topography (Set 5)		
Elevation	Mean	EarthEnv
Slope	Mean	EarthEnv